Electronic Supplementary Material (ESI) for ChemComm.

Electronic Supplementary Information

of

Mn (II) sub-nanometric sites stabilization in noble, N-doped carbonaceous materials for electrochemical CO_2 reduction

By J. Kossmann et al.

1. Experimental section

Materials: Uracil (98 %) was purchased from TCI chemical. Manganese (II) acetate was purchased from Sigma-Aldrich. Zinc chloride (98.5 %) is purchased from Acros organics. Potassium chloride (99.5 %) is from Pan Reac Applichem ITW reagents and Hydrochloric Acid (37 %) is from Roth. All materials are used as received.

Synthesis of the catalyst: To obtain the bare carbon material, uracil was grinded with KCl and $ZnCl_2$ in a 1:5:5 weight ratio and carbonized at 800 °C. The carbonization was performed under nitrogen atmosphere in a ceramic crucible with a ceramic cap. The powder mix was heated at 1 °C/min until 250 °C, hold for 2 h at that temperature and then heated at 1°C/min until 800 °C, and kept again for 2 h at that temperature. After letting cooling down, the carbon was washed 3 times with 1M HCl (24 h) and dried for 3 h at 70 °C.

Metal decoration was performed by simple impregnation and subsequent calcination of the as prepared carbon with a manganese (II) acetate solution in ethanol. In detail, 200 mg of the as prepared uracil carbon (URA) were added to 6 ml of a Mn (II) acetate solution (concentration in **Table S1**) and stirred for 1 h. The sample was then dried to remove ethanol. The dried impregnated URA powder was then calcined at 400 °C for 2 h under air atmosphere (1 °C/min).

CO_2 reduction reaction experiments: URA-MnX samples (10 mg) were dispersed in an ethanol solution (200 μL) containing 50μL of Nafion 117 solution (~ 5%) from Sigma-Aldrich, and sonicated until a homogeneous ink was obtained. The working electrodes were prepared by drop-casting 30 μL of the as-prepared ink on each side of a gas diffusion layer carbon paper (1.5 x 1 cm) (Spectracarb 2050-0550 from FuelCellStore) and allowed for solvent evaporation at room temperature. Then, the URA-MnX-based electrodes were vacuum dried overnight in order to remove all solvent traces. The electrochemical characterization was carried out with an electrochemical workstation (Gamry Interface 1000). CO_2RR was evaluated in a custom-made three-electrode H-cell configuration, separated by Nafion 117 membrane. As reference and counter electrodes $Ag/AgCl_{KCl\ sat.}$ and Pt foil were used respectively. 1M NaOH aqueous solution was used as electrolyte.

Characterization: Scanning electron microscopy (SEM) was performed with a LEO 1550-Gemini instrument from Zeiss. Samples were sputtered with gold/palladium 85/15% before measurement. SEM was coupled to a coupled Oxford Instrument energy-dispersive X-ray spectroscopy (EDX) analyser and elemental mapping was done. Using a PerkinElmer ICP-OES Optima 8000 ICP measurements ICP measurements were carried out. Fourier transformed infrared spectroscopy (FTIR) was performed in a Thermo Scientific Nicolet iS5 FT-IR spectrometer, using an attenuated total reflection iD5 accessory. Powder X-ray diffraction (XRD) pattern are performed using a Bruker D8 Advance instrument with Cu-Kα radiation. Scanning transmission electron microscopy (STEM) studies were performed using a double-Cs-corrected JEOL JEM-ARM200F (S)TEM equipped with a cold-field emission gun. The instrument was operated at 80 kV. Samples were suspended in ethanol using sonication for 15 min and then drop-casted on top of a lacey carbon covered Cu grid and let dry for another 15 min. Physisorption measurements with nitrogen and carbon dioxide at 77 K and 273 K were performed with a Quantachrome Quadrasorb SI instrument. Before measurements, all samples were degassed at 150 °C for 20 h under high vacuum. Brunauer-Emmett-Teller (BET) method was used for calculations of the specific surface area (S_{BET}) using nitrogen adsorption data ($P/P_0 < 0.2$) and the total pore volume (V_T) was calculated by the amount of nitrogen adsorbed at P/P_0=0.995. Nitrogen pore size distribution was calculated by using the Quenched Solid Density Functional Theory (QSDFT). Using a Thermo Fisher Scientific Escalab 250 Xi X-ray photoelectron spectroscopy (XPS) measurements were performed. ^{1}H-NMR spectra were recorded on Bruker Avance Ascen TM 400 MHz. Thermogravimetric analysis (TGA) was performed in a Pt crucible on a NETZSCHG 209 F1 from 25 °C to 1000 °C with nitrogen or synthetic air as carrier gas with a heating ramp of 10 K/min. EPR studies were conducted on a Bruker EMXnano benchtop X-Band EPR spectrometer. The spectra acquisition were acquired with a field centered at 3444.05 G, a receiver gain of 60 dB, a sweep width of 200 G, a modulation amplitude of 1.000 G and running 5 scans. Microwave attenuation was set at 10 dB. The samples were placed on flame-sealed EPR capillary tubes purchased from IntraMark (volume 50 µL, ID 0.86 mm).

High performance liquid chromatography (HPLC) was performed in order to analyse the liquid phase produces using a Dionex UltiMate 3000 UHPLC system, which consisted of an UltiMate 3000 RS pump, an UltiMate 3000 RS autosampler, an UltiMate 3000 RS column compartment and UltiMate 3000 RS Variable wavelength detector (Dionex Sortfon GmbH, Germany). A Rezex™ ROA-Organic Acid H^+ LC Column (300 x 7.8 mm) from Phenomenex was used. The samples were acidified with H_2SO_4 up to pH 2-3. The measurements were carried out with a H_2SO_4 solution (0.005 N) as mobile phase at 0.5 mL/min flow rate at 25 ºC. Catalytic performance tests were carried out under chronoamperometrie measurements. Gas products were detected by gas chromatography (GC) (Agilent 7890A) equipped with a MolSieve 5A column for H_2 analysis, while CO_2, CO, CH_4 and up to C4 hydrocarbons were analyzed with carboxene 1010 column.

2. Supporting Figures and Tables

Table S 1. Prepared manganese doped carbons with initial loading, real loading (*according to ICP measurements) and yield after impregnation and calcination.

Sample name	Mn (II) acetate (mg)	Final loading (wt%)*	Yield (wt%)
URA-Mn2	12.6	1.8	85.5
URA-Mn4	25.0	3.7	76.1
URA-Mn8	50.0	7.7	74.6

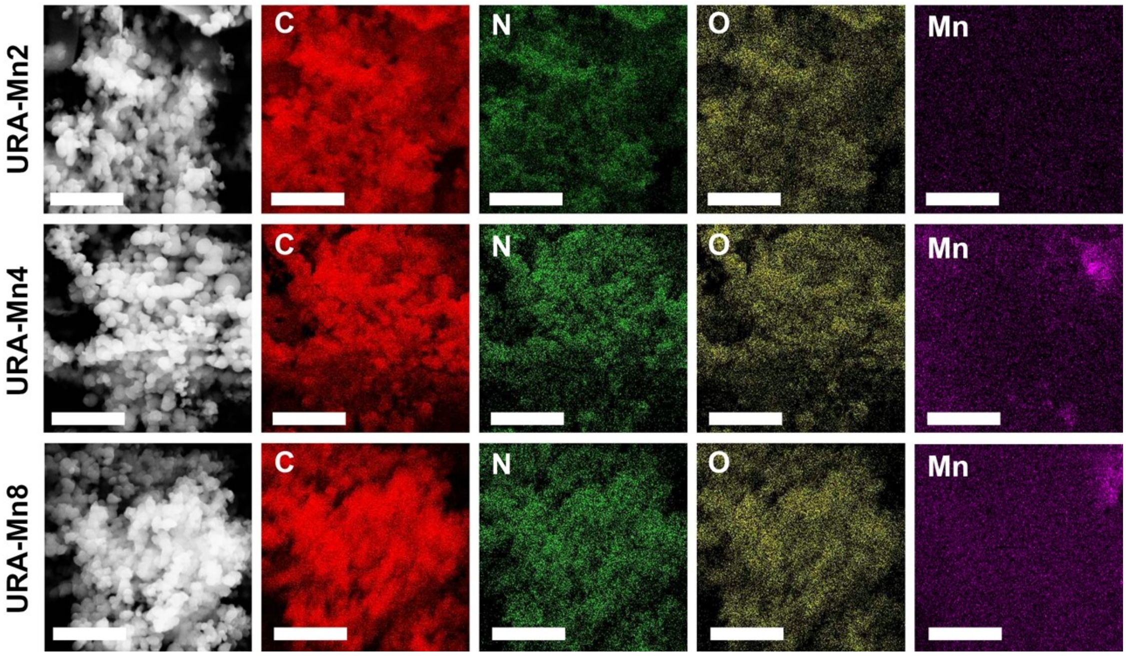

Figure S1. SEM-EDX elemental mapping of URA-Mn1, URA-Mn4 and URA-Mn8. Scale bars correspond to 1 µm.

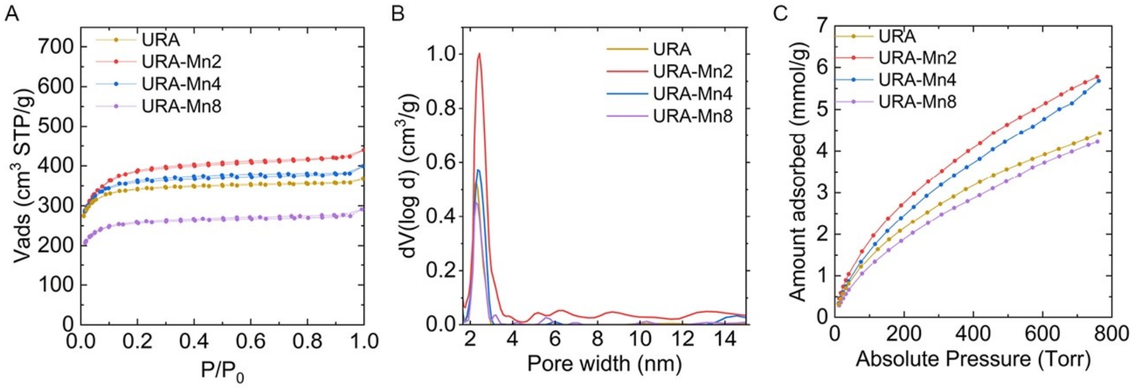

Figure S2. A) N_2 adsorption/desorption isotherms at 77 K, B) DFT pore size distribution obtained from nitrogen adsorption isotherms at 77 K, and C) CO_2 adsorption isotherms at 273 K of URA and URA-MnX materials.

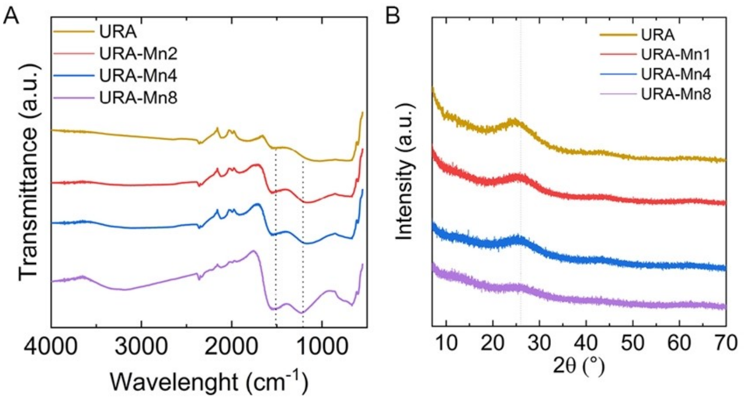

Figure S3. A) FTIR spectra and B) XRD pattern of URA and URA-MnX samples.

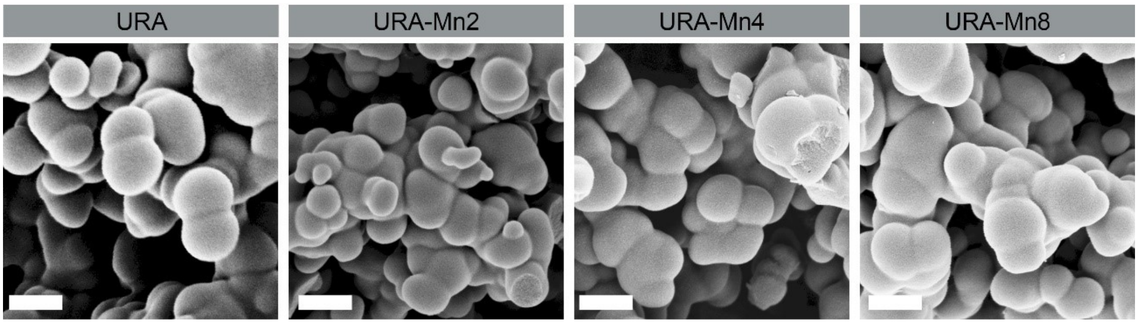

Figure S4. SEM images of URA and URA-MnX samples. Scale bar: 1µm.

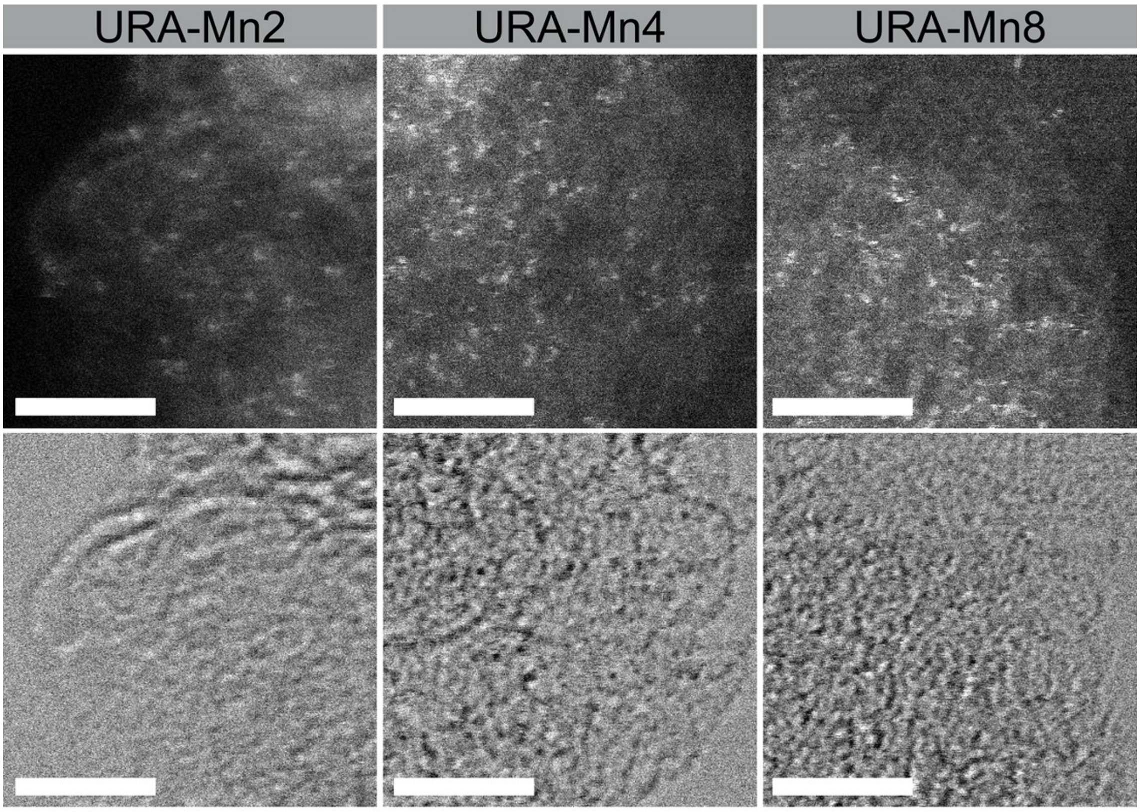

Figure S5. Dark and bright-field STEM of URA-Mn2, URA-Mn4 and URA-Mn8. Scale bar: 2 nm.

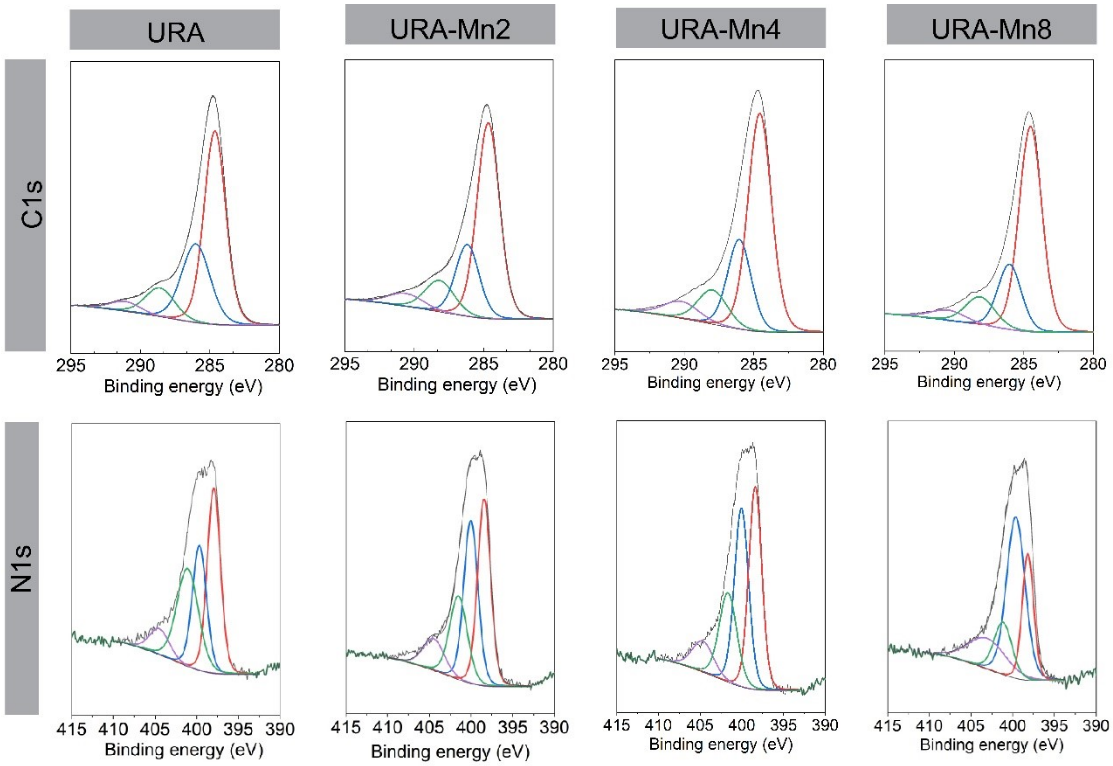

Figure S6. C1s and N1s deconvoluted XPS spectra of URA-MnX materials.

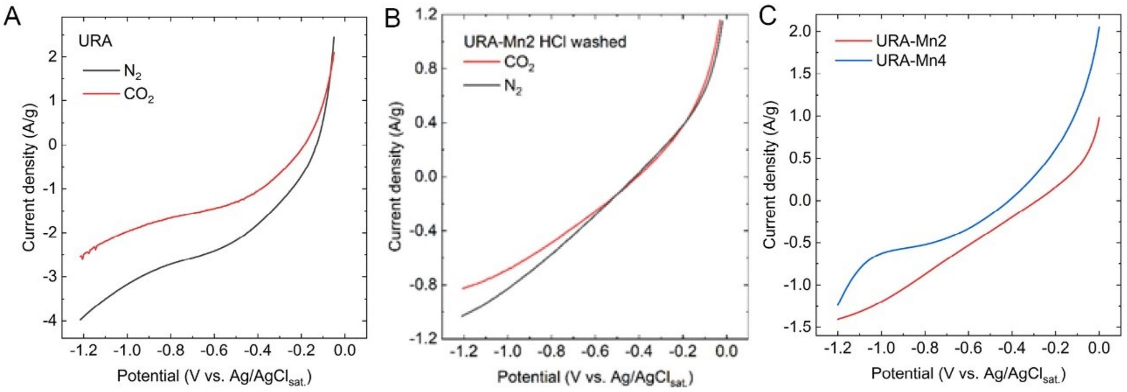

Figure S7. LSV curves of A) URA in N_2 (black) and CO_2 (red) saturated electrolyte und B)URA-Mn2 HCl washed in N_2 (black) and CO_2 (red) saturated electrolyte. C) URA-Mn2 (red) and URA-Mn4 (blue) CO_2 saturated electrolyte.

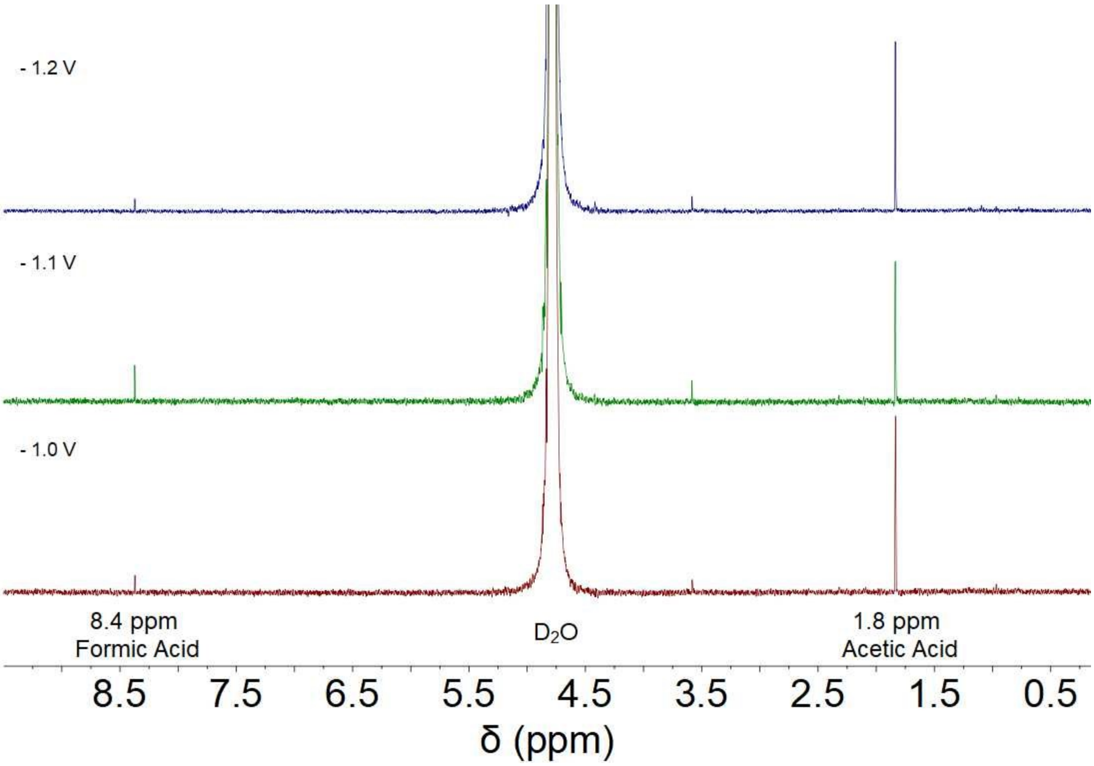

Figure S8. ^{1}H NMR of the electrolyte after 4 h chronoamperometrie at different potentials. Electrolyte was freeze dried and NMR measured in D_2O.

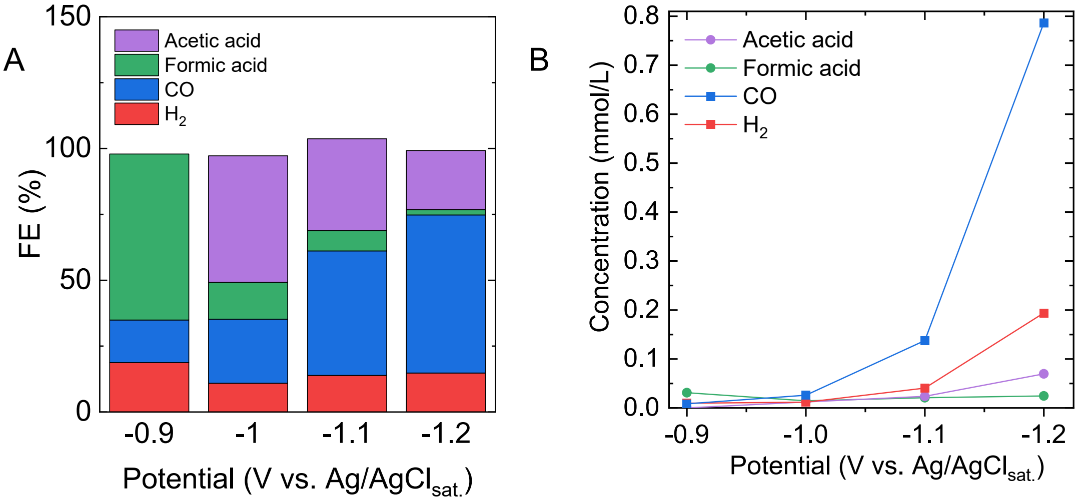

Figure S9. A) Faradaic efficiencies (%) and B) product concentrations (mol/L) applying different working voltages using URA-Mn2.

-